

# SQUARE TO HEXAGONAL LATTICE CONVERSION IN THE FREQUENCY DOMAIN

Xiangguo Li<sup>\*†</sup>      Bryan Gardiner<sup>‡</sup>      Sonya A. Coleman<sup>‡</sup>

<sup>†</sup>College of Information Science and Engineering, Henan University of Technology  
Zhengzhou, Henan, 450001 P.R. China e-mail:xianguoli@gmail.com

<sup>‡</sup>School of Computing and Intelligent Systems, University of Ulster, Magee, BT48 7JL, N. Ireland  
e-mail: b.gardiner@ulster.ac.uk, sa.coleman@ulster.ac.uk

## ABSTRACT

Currently, hexagonal image processing is mainly based on simulated data generated by square lattice conversions. For the evaluation of the conversion quality, this paper presents a method for ideal square to hexagonal lattice conversion. Based on the square lattice discrete-time Fourier transform (DTFT), the method first determines the values of the hexagonal discrete Fourier transform (HDFT), and performs the inverse HDFT to obtain the ideal conversion. This method provides a benchmark for evaluating other practical conversions and such evaluation is presented in this paper.

**Index Terms**— Hexagonal image processing, lattice conversion, DTFT, HDFT

## 1. INTRODUCTION

Although current digital imaging systems (including sensors, processing, and displays) are overwhelmingly based on the square lattice, the hexagonal lattice is indeed the theoretically optimal scheme. On the one hand, according to multidimensional sampling theory [1], as illustrated in Fig. 1(a), the hexagonal lattice is the optimal sampling scheme for circularly band-limited analog images and it will provide 13.4% fewer samples than the square lattice counterpart [2]. Since practical imaging systems generally use circularly symmetric lens and thus exhibit circularly low-pass nature, the hexagonal lattice is actually the optimal sampling scheme for practical sampled imaging systems. On the other hand, the hexagonal lattice is superior to the common square lattice in geometric properties, such as higher degree of symmetry, equal distance and uniform connectivity with its six neighbors [3], as shown in Fig. 1(b). Also, the hexagonal lattice is common in the structures of biological visual sensors, such as the compound eyes of insects [4] and the retina of human eyes [5], and thus hexagonal image processing has attracted researchers in bio-inspired image processing since the early days [6]. In recent years, hexagonal image processing research has spread to applications such as edge detection [7, 8], hexagonal Gabor filtering [9], ultrasound image processing [10], and adaptive beamforming [11].

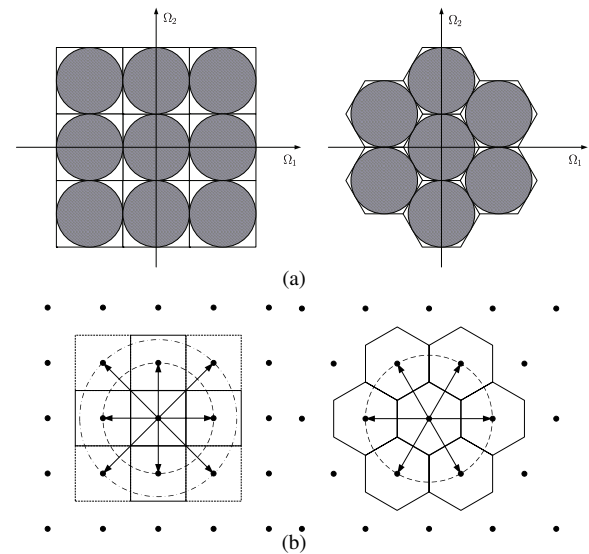


**Fig. 1.** Comparison between the square lattice and the regular hexagonal lattice. (a) illustrates the sampling efficiency and (b) illustrates the geometric properties.

However, due to the lack of practical imaging sensors at the present time, the hexagonal image processing research relies on the hexagonal lattice data obtained by converting from common square lattice data. In the theoretical aspects, Speake and Mersereau [12] have outlined the general lattice conversion theory with its matrix description, and they also developed the lattice conversion theory based on the 2-D multirate processing techniques [13]. Basically, the square to hexagonal lattice conversion is a common 2-D interpolation problem and can be easily understood from the reconstruction and resampling perspective. In practice, people often use simple interpolation kernels [14, 15], such as nearest-neighbor [16] and bilinear [17]. Also, spline-based approximation approaches have also been proposed, for example, in order to reduce the aliasing artifacts in the classical interpolation methods, Ville et al. [18] proposed the use of the hexagonal spline functions. Condat et al. [19] proposed a reversible conversion method, which decomposes the lattice conversion pro-

cess into three successive shear operations, and they implemented the method based on the 1-D fractional delay filters. Recently, Li et al. [20] proposed a simplified square to hexagonal lattice conversion approach, which performs 1-D interpolation along the horizontal direction only and thus can reduce the complexity as well as the computational costs.

Since current hexagonal image processing research is mainly performed on the data from square to hexagonal lattice conversion, and for a given application algorithm, data from different conversion methods may result in performance differences, i.e., the lattice conversion method may affect the performance of the following data processing components. A question naturally arises: how to evaluate the quality of a given lattice conversion method? We would need ground-truths that can be treated as ideally sampling the original analog images. This is the starting point of this paper.

To obtain the ground-truths, we need to perform the ideal square to hexagonal lattice conversion, i.e., the ideal interpolation. Theoretically, for the common square lattice sampling, the ideal interpolation kernel is the 2-D *sinc* function. In this paper, we propose to perform the ideal interpolation in the frequency domain, for which the bridge is the continuous nature of the discrete-time Fourier transform (DTFT). That is, for the hexagonal discrete Fourier transform (HDFT), we first determine each component value by computing the square lattice DTFT with the corresponding position, and then we perform the inverse HDFT to obtain the spatial data that are equivalent to the result from the spatial ideal interpolation.

The remainder of this paper is organized as follows. Section 2 introduces the 2-D sampling theory, and the image reconstruction and resampling framework. Then, Section 3 presents the proposed method for ideal square to hexagonal lattice conversion and Section 4 provides the experimental results and discussion. Finally, Section 5 concludes the paper.

## 2. PRELIMINARIES

### 2.1. 2-D signal sampling

Let  $x_a(t_1, t_2)$  denote a general 2-D analog signal, which is sampled with the rectangular lattice and the hexagonal lattice, respectively. First, the 2-D rectangular sampling can be expressed as  $x(n_1, n_2) = x_a(n_1 T_{r1}, n_2 T_{r2})$ , where  $T_{r1}$  and  $T_{r2}$  are the horizontal and vertical sampling intervals, respectively. If we assume that  $x_a(t_1, t_2)$  is rectangularly band-limited, as shown in Fig. 2(a), the sampling intervals to avoid aliasing must meet [2]:

$$T_{r1} \leq \frac{\pi}{W_{r1}} \text{ and } T_{r2} \leq \frac{\pi}{W_{r2}}, \quad (1)$$

where  $W_{r1}$  and  $W_{r2}$  are the horizontal and vertical bandwidths in radians, respectively.

The hexagonal sampling lattice is illustrated in Fig. 2(b), in which the two sampling directions are skewed with  $120^\circ$

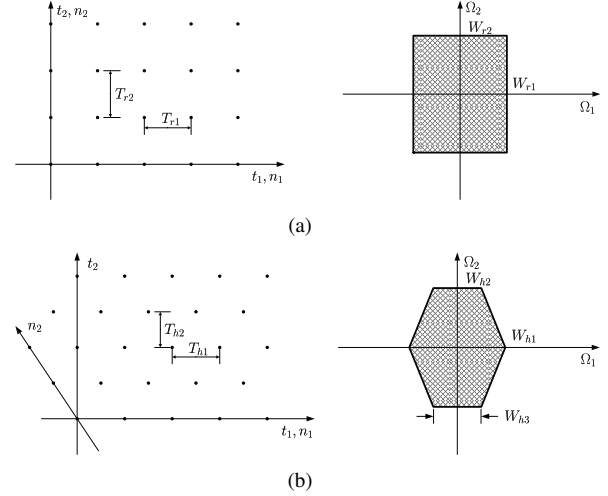


**Fig. 2.** Illustration of sampling lattices and the corresponding band regions (redrawn from [2]). (a) denotes the rectangular lattice and (b) denotes the hexagonal lattice.

(note that the two sampling intervals are defined in the two orthogonal directions). In this case, the sampling expression is given by  $x(n_1, n_2) = x_a((n_1 - \frac{1}{2}n_2)T_{h1}, n_2 T_{h2})$ . If we assume that  $x_a(t_1, t_2)$  is hexagonally band-limited with  $W_{h1}$ ,  $W_{h2}$ , and  $W_{h3}$  defined as in Fig. 2(b), the sampling intervals to avoid aliasing must fulfill [2]:

$$T_{h1} \leq \frac{4\pi}{2W_{h1} + W_{h3}} \text{ and } T_{h2} \leq \frac{\pi}{W_{h2}}. \quad (2)$$

Then, we consider the case where the 2-D analog signal is circularly band-limited. In this case, the rectangular lattice and the hexagonal lattice reduce to the square lattice and the regular hexagonal lattice, respectively. We define the circular band region as  $X_a(\Omega_1, \Omega_2) = 0$ , if  $\Omega_1^2 + \Omega_2^2 \geq W^2$ , where  $W$  is the radius. Then, to avoid aliasing exactly, the band regions in Fig. 2(a) and Fig. 2(b) should be able to hold the circular region exactly. Accordingly, the Nyquist sampling requirements are [2]

$$T_{s1} = \frac{\pi}{W} \text{ and } T_{s2} = \frac{\pi}{W} \quad (3)$$

for the square lattice and

$$T_{h1} = \frac{2\pi}{\sqrt{3}W} \text{ and } T_{h2} = \frac{\pi}{W} \quad (4)$$

for the regular hexagonal lattice.

### 2.2. Reconstruction and resampling

It is easy to understand the lattice conversion in the context of the reconstruction and resampling framework. Given the sampling intervals for the square lattice as  $T_{s1}$  and  $T_{s2}$ , where  $T_{s1}$  and  $T_{s2}$  are equal, and also the sampling intervals for the

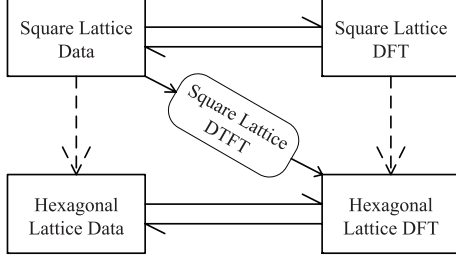


**Fig. 3.** Illustration of the motivation for the proposed method.

regular hexagonal lattice  $T_{h1}$  and  $T_{h2}$ . Besides, we assume that the two lattices fulfill the critical sampling requirements exactly.

Then, we start with the square lattice samples  $x_s(n_1, n_2) = x_a(n_1T_{s1}, n_2T_{s2})$ , assume to reconstruct the analog image  $x_r(t_1, t_2)$ , and then resample to obtain the hexagonal lattice data  $x_h(k_1, k_2) = x_r((k_1 - \frac{1}{2}k_2)T_{h1}, k_2T_{h2})$ . To reconstruct the analog image, we denote the reconstruction filter as  $h_r(t_1, t_2)$ , and the reconstruction process is

$$x_r(t_1, t_2) = \sum_{n_1} \sum_{n_2} x_s(n_1, n_2) h_r(t_1 - n_1T_{s1}, t_2 - n_2T_{s2}), \quad (5)$$

which is a shift-variant convolution.

Finally, we perform the hexagonal lattice resampling. According to the assumption, there is no need to apply any anti-aliasing filter before the resampling, thus the hexagonal lattice data can be obtained by

$$\begin{aligned} x_h(k_1, k_2) &= x_r((k_1 - \frac{1}{2}k_2)T_{h1}, k_2T_{h2}) \\ &= \sum_{n_1} \sum_{n_2} x_s(n_1, n_2) h_r((k_1 - \frac{1}{2}k_2)T_{h1} - n_1T_{s1}, \\ &\quad k_2T_{h2} - n_2T_{s2}). \end{aligned} \quad (6)$$

It is clear that the lattice conversion is a 2-D interpolation problem.

### 3. FREQUENCY DOMAIN CONVERSION

For the proposed ideal square to hexagonal lattice conversion method, the motivation is illustrated in Fig. 3. Given the square lattice data  $x_s(n_1, n_2)$ , we want to obtain the perfect hexagonal lattice data  $x_h(k_1, k_2)$ . For both the square lattice and the hexagonal lattice, their spatial samples are equivalent to their frequency domain samples obtained from the corresponding DFTs, i.e., we can perfectly convert the spatial data to the discrete spectrum, and vice versa. Therefore, if we assume  $h_r(t_1, t_2)$  is the ideal reconstruction filter, we can apply (6) to complete the ideal square to hexagonal lattice conversion in either the spatial domain or the frequency domain, as indicated by the dash-line arrows in Fig. 3.

**Table 1.** The PSNR (in dB) results of the experiments.

images	“nearest-neighbor”	“bilinear”	“bicubic”
“IM002.tif”	35.3313	42.0143	44.5362
“IM023.tif”	34.2255	39.4381	41.9161
“IM052.tif”	31.9119	37.0771	38.6962
“IM065.tif”	31.7340	37.6169	39.8090
“IM077.tif”	34.0174	38.5320	40.2184
“IM014.tif”	37.3021	42.0640	44.4166
“IM035.tif”	30.1346	34.4484	36.2190
“IM041.tif”	29.9663	35.1178	37.2844
“IM127.tif”	30.7593	36.8227	39.8188
“IM130.tif”	39.9978	45.2878	46.8872

We notice that, although a digital signal is discrete against the continuous original signal, its spectrum is still continuous, for which the relation is through the DTFT. Therefore, since the DFT is the sampling of the DTFT in the frequency domain, we can determine each value of the DFT by computing the DTFT, and in this paper we propose to determine the exact values of the hexagonal lattice DFT by the square lattice DTFT. Then, we perform the inverse HDFT and obtain the ideal conversion results that are equivalent to the spatial domain ideal interpolation. In this approach, unlike the common way that we obtain the spectrum from the spatial domain data, we first determine the spectrum and then obtain the spatial domain data. Note that the proposed method is for evaluation purposes only and not for practical square to hexagonal lattice conversion, thus its computational efficiency is not a main concern.

### 4. RESULTS AND DISCUSSION

We implemented the proposed method and used it to evaluate the commonly used interpolation kernels, namely the “nearest-neighbor”, “bilinear”, and “bicubic”. These three kernels are also common in practical square to hexagonal lattice conversion. In the experiments, we chose 10 color images from the Laurent Condat’s Image Database [21], as shown in Fig. 4. For each test image, we performed the conversion with the proposed method and the three interpolation kernels separately, then computed the peak signal-to-noise ratio (PSNR) of each kernel against the ground-truth, and the results were listed in Table 1.

The PSNR results are consistent with our knowledge about these three kernels, i.e., “nearest-neighbor” performs worst, “bilinear” performs better, and “bicubic” performs best. For the “bicubic” kernel, the results are approximately 40 dB, thus it could obtain good approximation for general applications. Also, the image texture has an effect on the interpolation results, which is evident from the difference in PSNR results in Table 1 and also demonstrated by the visual effectiveness with three typical images in Fig. 5.



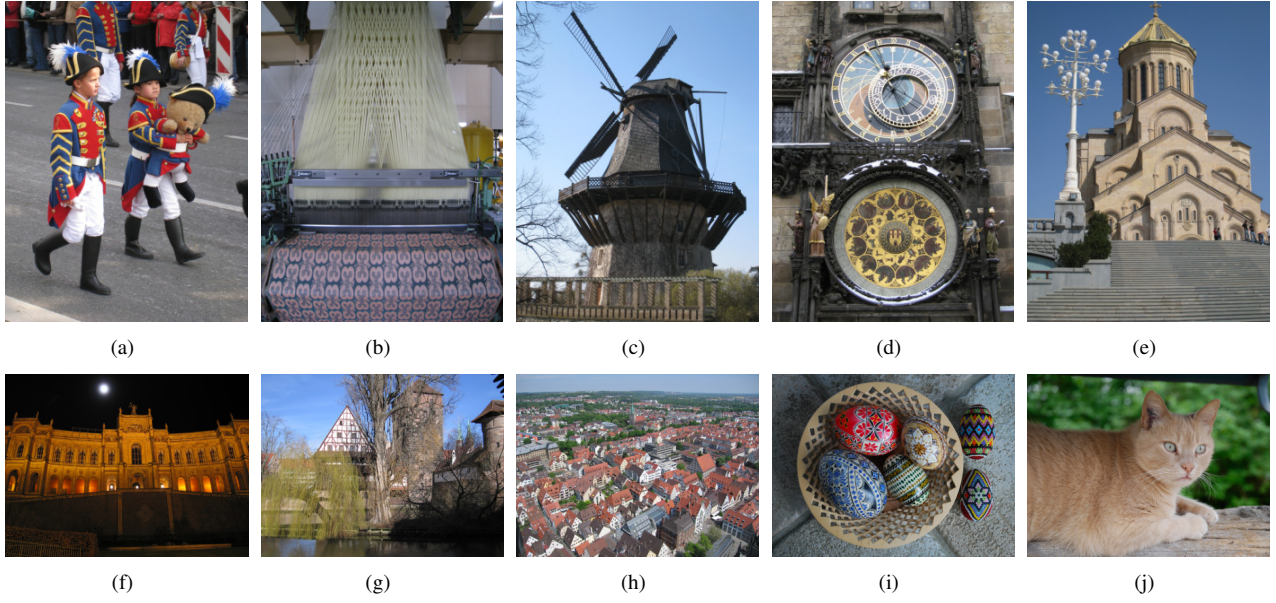


**Fig. 4.** Test images used in the experiments. From (a) through (j): “IM002”, “IM023”, “IM052”, “IM065”, “IM077”, “IM014”, “IM035”, “IM041”, “IM127”, “IM130”, respectively.



**Fig. 5.** Illustration of the absolute errors ( $\times 10$  and inverted) with three test images. Each row, from left to right: test image, ideally converted image, and then the absolute errors of “nearest-neighbor”, “bilinear”, and “bicubic”, respectively.

## 5. CONCLUSION

In this paper, we presented a method for ideal square to hexagonal lattice conversion. The method was based on the continuous nature of the DTFT. Then, we proposed to use the square

lattice DTFT for the exact values of the HDFT, and performed the inverse HDFT to obtain the expected ideal conversion result. The method can be used to benchmark other practical square to hexagonal lattice conversion methods and results.

## 6. REFERENCES

- [1] Daniel P. Petersen and David Middleton, "Sampling and reconstruction of wave-number-limited functions in N-dimensional euclidean spaces," *Information and Control*, vol. 5, no. 4, pp. 279–323, 1962.
- [2] R.M. Mersereau, "The processing of hexagonally sampled two-dimensional signals," *Proceedings of the IEEE*, vol. 67, no. 6, pp. 930–949, 1979.
- [3] Xiangguo Li, "Storage and addressing scheme for practical hexagonal image processing," *Journal of Electronic Imaging*, vol. 22, no. 1, pp. 010502, 2013.
- [4] Kurt J.A Vanhoutte, Kristel F.L Michielsens, and Doekele G Stavenga, "Analyzing the reflections from single ommatidia in the butterfly compound eye with voronoi diagrams," *Journal of Neuroscience Methods*, vol. 131, no. 1–2, pp. 195–203, 2003.
- [5] Christine A. Curcio, Kenneth R. Sloan, Robert E. Kalina, and Anita E. Hendrickson, "Human photoreceptor topography," *The Journal of Comparative Neurology*, vol. 292, no. 4, pp. 497–523, 1990.
- [6] M.J.E. Golay, "Hexagonal Parallel Pattern Transformations," *IEEE Transactions on Computers*, vol. C-18, no. 8, pp. 733–740, aug 1969.
- [7] K. Mostafa, J. Y. Chiang, and I. Her, "Edge-detection method using binary morphology on hexagonal images," *The Imaging Science Journal*, vol. 63, no. 3, pp. 168–173, 2015.
- [8] Bryan Gardiner, Sonya Coleman, and Bryan Scotney, "Multiscale Edge Detection using a Finite Element Framework for Hexagonal Pixel-based Images," *IEEE Transactions on Image Processing*, vol. 25, no. 4, pp. 1849 – 1861, 2016.
- [9] S. Veni and K. A. Narayanankutty, "Vision-based hexagonal image processing using Hex-Gabor," *Signal, Image and Video Processing*, vol. 8, no. 2, pp. 317–326, 2014.
- [10] Sonia H. Contreras-Ortiz and Martin D. Fox, "Hexagonal filters for ultrasound images," *Journal of Electronic Imaging*, vol. 23, no. 4, pp. 043022, 2014.
- [11] Jose Francisco de Andrade, Marcello L. R. de Campos, and Jose Antonio Apolinario, "L1-Constrained Normalized LMS Algorithms for Adaptive Beamforming," *IEEE Transactions on Signal Processing*, vol. 63, no. 24, pp. 6524–6539, 2015.
- [12] T. Speake and R. Mersereau, "An interpolation technique for periodically sampled two-dimensional signals," in *IEEE International Conference on Acoustics, Speech, and Signal Processing (ICASSP'81)*, 1981, vol. 6, pp. 1010–1013.
- [13] R. Mersereau and T. Speake, "The processing of periodically sampled multidimensional signals," *IEEE Transactions on Acoustics, Speech, and Signal Processing*, vol. 31, no. 1, pp. 188–194, 1983.
- [14] Innchyn Her and C.T. Yuan, "Resampling on a pseudo-hexagonal grid," *CVGIP: Graphical Models and Image Processing*, vol. 56, no. 4, pp. 336–347, 1994.
- [15] Bryan Gardiner, Sonya Coleman, and Bryan Scotney, "Comparing Hexagonal Image Resampling Techniques with Respect to Feature Extraction," in *14th International Machine Vision and Image Processing Conference*, 2011.
- [16] J Serra and B Laÿ, "Square to hexagonal lattices conversion," *Signal Processing*, vol. 9, no. 1, pp. 1–13, 1985.
- [17] Xiangjian He, Jianmin Li, and Tom Hintz, "Comparison of Image Conversions Between Square Structure and Hexagonal Structure," in *9th international conference on Advanced concepts for intelligent vision systems*, 2007, pp. 262–273.
- [18] Dimitri Van De Ville, Wilfried Philips, and Ignace Lemahieu, "Least-squares spline resampling to a hexagonal lattice," *Signal Processing: Image Communication*, vol. 17, no. 5, pp. 393–408, 2002.
- [19] Laurent Condat, Dimitri Van De Ville, and Brigitte Forster-Heinlein, "Reversible, fast, and high-quality grid conversions.," *IEEE transactions on image processing*, vol. 17, no. 5, pp. 679–693, 2008.
- [20] Xiangguo Li, B. Gardiner, and S.A. Coleman, "Square to Hexagonal Lattice Conversion Based on One-Dimensional Interpolation," in *2016 Sixth International Conference on Image Processing Theory, Tools and Applications (IPTA)*, 2016, pp. 1–6.
- [21] Laurent Condat, "Laurent Condat's Image Database," <http://www.gipsa-lab.grenoble-inp.fr/~laurent.condat/imagebase.html>.